Materials Science Forum
ISSN: 1662-9752, Vol. 930, pp 405-410
doi:10.4028/www.scientific.net/MSF.930.405

Submitted: 2018-01-22
Accepted: 2018-01-29
Online: 2018-09-14

Study of the Correlation between Microstructure and Corrosion Resistance of the AZ91D Magnesium Alloy

Renato Altobelli Antunes[1,a*], Mara Cristina Lopes de Oliveira[2,b], Lucas Costa de Castro Ferraz[1,c], Letícia dos Reis Gonçales[1,d], Olandir Vercino Correa[3,e]

[1]Universidade Federal do ABC (UFABC), Centro de Engenharia Modelagem e Ciências Sociais Aplicadas (CECS) -Santo André – SP – Brazil - 09210-580 – renato.antunes@ufabc.edu.br

[2]Electrocell Ind. Com. de Equip. Elétricos LTDA, CIETEC – São Paulo – SP – Brazil - 05508-000

[3]Instituto de Pesquisas Energéticas e Nucleares (IPEN/CNEN-SP), Centro de Ciência e Tecnologia de Materiais (CCTM), São Paulo – SP – Brazil

[a]renato.antunes@ufabc.edu.br, [b]mara.oliveira@usp.br, [c]ferraz.lcc@live.com, [d]leticiareis.eng@gmail.com, [e]ovcorrea@ipen.br

Keywords: AZ91D, beta phase, precipitates distribution, corrosion resistance

Abstract. The aim of the present work was to study the influence of beta phase precipitates content and distribution on the corrosion behavior of the AZ91D magnesium alloy, using samples subjected to solution annealing and aging. The morphology of the beta phase was observed using optical microscopy and scanning electron microscopy. The volume fraction of each phase was also determined. Potentiodynamic polarization tests and immersion tests were carried out, indicating an increase of the corrosion resistance with the volume fraction of the beta phase and its distribution on the grain boundaries of the alpha-phase. Solution annealed samples were more susceptible to corrosion.

Introduction

Pure magnesium has limited engineering applications due to its intrinsic high chemical reactivity [1]. The corrosion resistance and mechanical strength can be improved by proper addition of alloying elements [2]. The AZ series with Al and Zn additions has found widespread use in the automobile industry due to a good strength to weight ratio and easy manufacturing by die casting processes [3]. Microstructure is a key factor for the corrosion behavior of cast magnesium alloys. The AZ91D alloy presents a binary structure, consisting mainly of the magnesium matrix (α-Mg) and the aluminum-rich β-phase ($Mg_{17}Al_{12}$) [4]. The β-phase is cathodic with respect to the magnesium matrix and is reported to play a central role in the corrosion resistance of the AZ91D alloy [5]. Characteristics such as morphology and volume fraction have a strong influence on the corrosion properties of the alloy, being affected by specific heat treatments [6]. Esmaily et al. [7] observed that the β-phase can give rise to a barrier effect against AZ91D corrosion, depending on its size, morphology and fraction. Ambat et al. [8] highlighted the beneficial effect of the formation of a close network of β particles to slow down dissolution of the AZ91 alloy as well as the importance of its cathodic character with respect to the α-phase which is mainly related to the aluminum content in the intermetallic β phase. In this respect, this phase may either accelerate the dissolution of the alloy or act as a barrier against corrosion. Current literature points to conflicting results for the effect of the β phase on the corrosion behavior of the AZ91D alloy. There is, therefore, a demand for additional work on this subject in order to gain further understanding on this subject. The aim of the present work was to investigate the effect of β phase distribution and morphology on the corrosion behavior of the AZ91D alloy.

Experimental Procedure

Material and Heat Treatments

Die cast AZ91D ingot was kindly provided by Rima Industrial Magnésio (Brazil). Small rectangular pieces with an area of approximately 1 cm^2 were cut from the ingot. The samples were subjected to solution annealing at 445°C for 24 h in a tubular furnace under argon atmosphere. Next, the samples were quenched in water. In order to obtain different microstructures, the samples were aged at 200 °C for three different periods: 2 h, 6 h and 24 h in a tubular furnace under argon atmosphere.

Electrochemical tests. Samples surfaces were ground with waterproof SiC abrasive papers to 2400 grit and washed with deionized water. A conventional three-electrode cell was used for the electrochemical tests with a platinum wire as the counter-electrode, Ag/AgCl as reference and the AZ91D samples as the working electrodes. The open circuit potential (OCP) was monitored for 1800 s. Next, potentiodynamic polarization curves were acquired in the potential range from -300 mV versus the OCP up to 0 $V_{Ag/AgCl}$ with a scanning rate of 1 $mV.s^{-1}$. A 3.5 wt.% NaCl solution at room temperature was used as the electrolyte. The tests were carried out in triplicate using an Ivium nStat potentiostat/galvanostat.

Immersion test. Immersion tests were conducted for 16 days in 3.5 wt.% NaCl solution at room temperature, according to ASTM –G31. The samples were weighed before immersion. After immersion, the samples were cleaned in an aqueous solution consisting of 200 $g.L^{-1}$ CrO_3 and 10 $g.L^{-1}AgNO_3$. Next, the samples were washed with deionized water, dried and weighed again. The corrosion rate was estimated by weight loss measurements, following equation (1), where w is the weight loss, w_i is the initial weight and w_f is the final weight, after removal of corrosion products. Five samples were tested for each heat treatment condition.

$$w = \frac{\left(w_i - w_f\right)}{w_i} \tag{1}$$

Microstructural analysis. Specimens for microstructural examination were embedded in bakelite and ground to grit 2400, following polishing with diamond paste up to 1 μm. The microstructure was revealed by chemical etching in a solution consisting of ethanol, nitric acid, acetic acid and deionized water for 45 s. Microstructure examination was performed using optical microscopy and scanning electron microscopy (SEM, Hitachi TM3000) coupled with an energy dispersive X-ray spectroscopy (EDS) detector for chemical microanalysis.

Results and Discussion

Microstructural analysis. The microstructure of the as-received AZ91D alloy is shown in Fig. 1. Fig1a shows an optical micrograph of the alloy, consisting of a dendritic α-Mg phase, a eutectic phase and islands of the intermetallic β-phase. The SEM micrograph in Fig. 1b reveals the presence of white-colored phases which have been identified as Mn-rich precipitates by EDS (spectrum not shown) The composition of each phase was confirmed by EDS analysis. SEM micrographs of the solution annealed (SA) and aged microstructures are shown in Fig. 2. Solution annealing dissolved the β-phase, leaving mainly the magnesium matrix and Mn-rich precipitates. After aging, the β-phase precipitated as indicated by the light-grey regions in Figs. 2b, 2c and 2d. Depending on the aging time, different β-phase morphologies were obtained. For the 2 h-aging precipitation is discontinuous. After aging for 6 h the β-phase precipitated more continuously along the grain boundaries of the matrix. Aging for 24 h promoted the formation of β precipitates along the grain boundaries with a mixed continuous and discontinuous morphology, and also inside the grains. In this respect, the aging treatment led to precipitation of β-phase along the grain boundaries, creating a network of Al-rich β particles which also formed inside the α-grains after aging for 24 h.

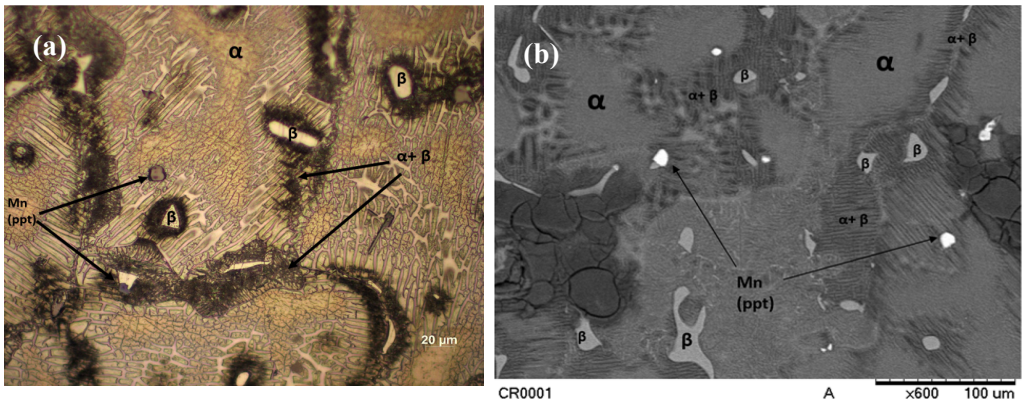

Fig. 1. Microstructure of the as-received AZ91D alloy: a) optical micrograph; b) SEM micrograph.

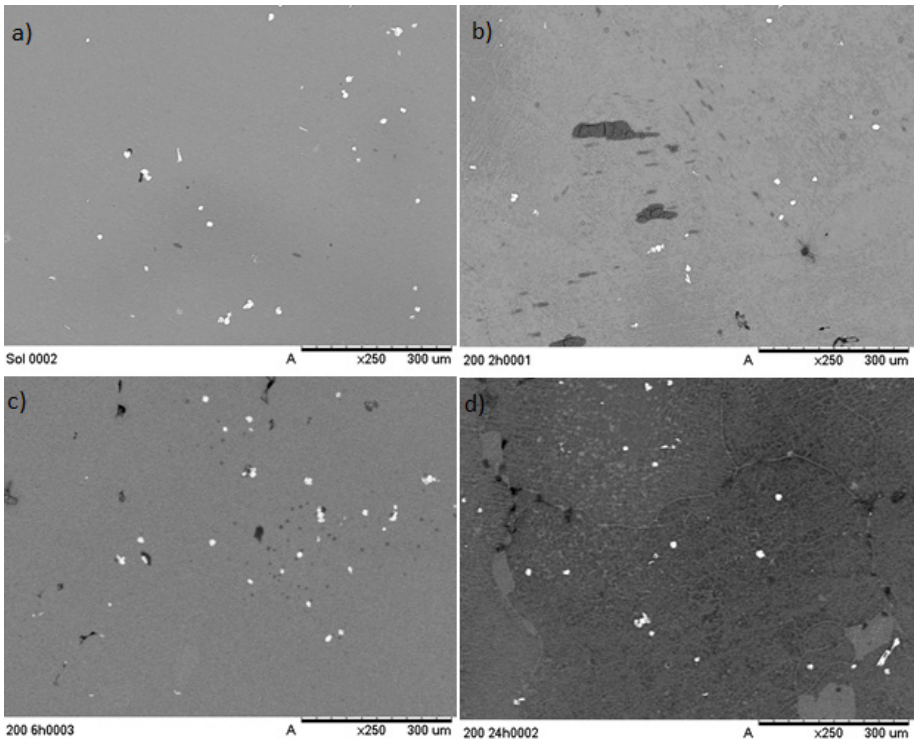

Fig. 2. SEM micrographs of the AZ91D after solution annealing (a) and aging for: (b) 2 h; (c) 6 h and (d) 24 h.

Quantification of the different phases was carried out based on the SEM micrographs by using the ImageJ software. The volume fraction of each phase was calculated considering an approximate uniaxial morphology and assuming equivalence between this parameter and the corresponding surface fraction on the micrographs. The results are shown in Table 1. The fraction of Mn-rich precipitates was not significantly affected by the heat treatments whereas the β-phase was severely affected. After solution annealing, the β-phase was almost completely dissolved. Aging promoted precipitation of the β-phase which was enhanced for longer treatment times.

Table 1. Volume fraction analysis for the phases of the AZ91D alloy in the as-received condition and subjected to different heat treatments.

Condition	Microconstituent	Volume fraction
As-received	Eutectic (α+β)	0.178
	Mn-rich	0.006
	β	0.032
Solution annealed	Mn-rich	0.008
	β	0.002
Aged-2h	Mn-rich	0.007
	β	0.006
Aged-6h	Mn-rich	0.006
	β	0.010
Aged-24h	Mn-rich	0.008
	β	0.011

Corrosion tests. Representative potentiodynamic polarization curves of the AZ91D alloy subjected to different heat treatments are shown in Fig. 3. The curves were obtained in 3.5 wt.% NaCl solution at room temperature.

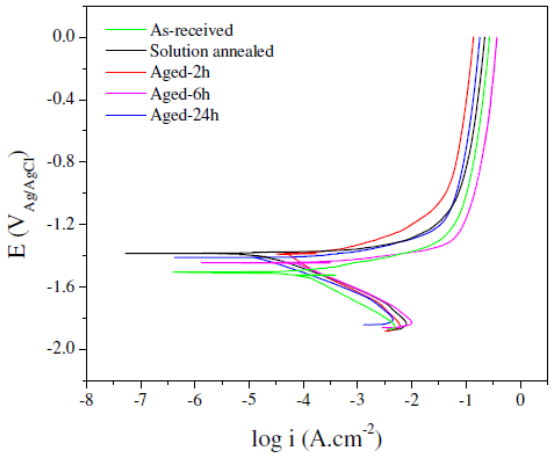

Fig. 3. Potentiodynamic polarization curves of the AZ91D alloy in 3.5 wt.% NaCl solution at room temperature.

Values of corrosion potential (E_{corr}), corrosion current density (i_{corr}) and cathodic Tafel slopes (b_c) were determined from the polarization curves using the Tafel extrapolation method, considering only the cathodic branch. The results are displayed in Table 2. The polarization curves do not show any distinguishable passivity. The cathodic branches almost coincide for all the curves, suggesting that the cathodic reactions are not affected by the heat treatments. There is a tendency of increasing the corrosion potential and reducing the anodic current densities for the heat treated material. This trend can be perceived by comparing the value of E_{corr} of the as-received material with those of the solution annealed and aged specimens. The variation of i_{corr} could not be directly related to microstructural changes.

Table 2. Electrochemical parameters determined from the potentiodynamic polarization curves of the AZ91D alloy subjected to different heat treatments.

Parameter	Condition				
	As-received	Solution annealed	Aged-2h	Aged-6h	Aged-24h
E_{corr} ($V_{Ag/AgCl}$)	-1.56±0.02	-1.39±0.01	-1.40±0.01	-1.38±0.04	-1.40±0.04
b_c (mV/decade)	-185±6	-129±12	-171±39	-126±6	-136±6
i_{corr} (mA/cm²)	0.09±0.02	0.06±0.04	0.03±0.01	0.10±0.04	0.02±0.01

It is seen from Table 2 that there was a trend of decreasing the values of i_{corr} for the heat treated alloy when compared to the as-cast microstructure. However, this trend does not apply to the specimens aged for 6 h. Furthermore, if one considers the standard deviations associated with the i_{corr} values, it is also difficult to perceive a clear relationship between microstructure and the corrosion current density determined using the Tafel extrapolation method. Similar effects have been reported by other authors [9,10]. Recently, Choi and Kim [11] have found that the i_{corr} value of AZ31 alloy did not agree with the corrosion rate determined from weight loss measurements which yielded more reliable results. The unclear nature of i_{corr} was attributed to the negative difference effect (NDE) [12]. Immersion tests were carried out to gain further understanding on the correlation between microstructure and corrosion behavior. The results are shown in Table 3. Solution annealing was clearly detrimental to the corrosion resistance of the AZ91D alloy, yielding the highest weight loss. After aging, the weight loss was reduced to values which were compatible with the as-received condition but lower in the average. The β phase is present either in the as-received or aged conditions, being continuously distributed along the grain boundaries of the matrix or discontinuous but refined inside the α grains for the aged samples. For the as-cast material, in turn, the β phase forms larger particles and is also present as part of the eutectic microconstituent (α+β).The highest weight loss of the solution-annealed material confirms that the β phase plays a beneficial role on the corrosion resistance of the AZ91D alloy. Furthermore, the β phase morphology exerts a marked influence on the overall weight loss of this material. Our results point that corrosion resistance is higher when it is distributed along grain boundaries or inside the grains of the α matrix, forming a network of β particles (microstructure characteristic of the aged condition) than when it is mostly isolated and part of the eutectic constituent (microstructure characteristic of the as-received condition). This effect has been observed by Ambat et al.[8].

Table 3. Weight loss results for the AZ91D alloy after 16 days of immersion in 3.5 wt.% NaCl solution at room temperature.

Condition	Weight loss (%)
As-received	0.66% ± 0.36%
Solution annealed	4.44% ± 2.05%
Aged-2h	0.31% ± 0.24%
Aged-6h	0.40% ± 0.22%
Aged-24h	0.39% ± 0.04%

Conclusions

Solution annealing dissolved the β-phase, leaving a microstructure consisting of α-Mg. After aging, the β-phase precipitated along grain boundaries and also inside the grains of the matrix, forming a continuous network that was enhanced for longer treatment times. The microstructure effect on the corrosion resistance of the AZ91D alloy could not be perceived by potentiodynamic polarization tests. Weight loss measurements, in turn, indicated that the β-phase morphology influenced the material's corrosion behavior. Solution-annealed samples presented the highest weight loss. The presence of the β-phase in the as-cast and aged microstructures decreased the weight loss with respect to the solution annealing condition. The formation of a continuous network of β-phase particles after aging leads to a barrier effect against corrosion.

Acknowledgements

Authors are thankful to Rima Industrial Magnésio (Brazil).

References

[1] M. Alvarez-Lopez, M.D. Pereda, J.A. Del Valle, M. Fernandez-Lorenzo, M.C. Garcia-Alonso, O.A. Ruano, M.L. Escudero: Acta Biomater. Vol. 6 (2010), p. 1763.
[2] M. Mondet, E. Barraud, S. Lemonnier, J. Guyon, N. Allain, T. Grosdidier: Acta Mater. Vol. 119 (2016), p. 55.
[3] D. Zander, C. Schnatterer: Corros. Sci. Vol. 98 (2015), p. 291.
[4] N.N. Aung, W. Zhou: J. Appl. Electrochem. Vol. 32 (2002), p.1397.
[5] G. Song, A. Atrens, M. Dargusch: Corros. Sci. Vol. 41 (1999), p. 249.
[6] M. Laleh, F. Kargar: J. Alloys Compd. Vol. 509 (2011), p. 9150.
[7] M. Esmaily, N. Motazavi, J.E. Svensson, M. Halvarsson, D.B. Blücher, A.E.W. Jarfors, M. Wessén, L.G. Johansson: J. Electrochem. Soc. Vol. 162 (2015), p. C311.
[8] R. Ambat, N. Aung, W. Zhou: J. Appl. Electrochem. Vol. 30 (2000), p. 865.
[9] Z. Shi, M. Liu, A. Atrens: Corros. Sci. Vol. 52 (2010), p. 579.
[10] G. Song: Adv. Eng. Mater. Vol. 7 (2005), p. 563.
[11] H.Y. Choi, W.J. Kim: J. Alloys Compd. Vol. 664 (2016), p. 25.
[12] T.R. Thomaz, C.R. Weber, T. Pelegrini Jr., L.F.P. Dick, G. Knömschild: Corros. Sci. Vol. 52 (2010), p. 2235.